



**HAL**  
open science

# Influence of Process Parameters on the Gas Phase Polymerization of Ethylene: RSM or ANN Statistical Methods?

Niyi B Ishola, Timothy Mckenna

► **To cite this version:**

Niyi B Ishola, Timothy Mckenna. Influence of Process Parameters on the Gas Phase Polymerization of Ethylene: RSM or ANN Statistical Methods?. *Macromolecular Theory and Simulations*, In press, 10.1002/mats.202100059 . hal-03439649

**HAL Id: hal-03439649**

**<https://hal.science/hal-03439649>**

Submitted on 22 Nov 2021

**HAL** is a multi-disciplinary open access archive for the deposit and dissemination of scientific research documents, whether they are published or not. The documents may come from teaching and research institutions in France or abroad, or from public or private research centers.

L'archive ouverte pluridisciplinaire **HAL**, est destinée au dépôt et à la diffusion de documents scientifiques de niveau recherche, publiés ou non, émanant des établissements d'enseignement et de recherche français ou étrangers, des laboratoires publics ou privés.

# **Influence of Process Parameters on the Gas Phase Polymerization of Ethylene: RSM or ANN Statistical Methods?**

*Niyi B. Ishola, Timothy F.L. McKenna\**

CP2M-UMR 5128, Université de Lyon, Bâtiment CPE-Lyon, 43 Blvd du 11 Novembre 1918, F-69616 Villeurbanne, France

\*timothy.mckenna@univ-lyon1.fr

## **Abstract**

The direct and interactive effects of process variables, including the use of *iso*-pentane as an inert condensing agent (ICA), on the rate of polymerization and main physical properties of linear low-density polyethylene (LLDPE) were studied using two different statistical methods. RSM based on a three level five factor Box-Behnken design (BBD) was used to generate the number of experimental runs. The generated dataset was used to develop the RSM and artificial neural network (ANN) models. The effect of the input on the dependent variables was studied using the 3D response surface of the developed RSM model. The developed models were statistically analysed and compared to determine their performance capability. The ANN model marginally outperformed the RSM model based on the computed statistical parameters but provides less information on the variable interactions.

**Key Words:** LLDPE; process parameters; experimental design; statistical methods.

## **1.0 Introduction**

Gas phase ethylene polymerization on supported Ziegler-Natta or metallocene catalysts in fluidized bed reactors (FBR) is the most widely used process to produce linear low-density polyethylene (LLDPE). However, despite the ubiquity of this process, and the progress made in developing (semi) mechanistic models of the polymerization kinetics and basic polymer properties, there remains much to be elucidated in terms of fundamental understanding of both the precise kinetic mechanism defined by the catalyst formulation on the one hand, and the impact of certain process parameters and operating conditions on the other. In the current paper, we will concern ourselves with the latter problem: the impact of process parameters.

The complexity of the physical processes involved means that it can be difficult to identify all of the potentially important effects that changes in operating conditions might have, and particularly interactions between different process parameters. This situation might

be further complicated by the way in which many laboratory scale experiments are run in both industrial and academic research laboratories. In fact, it is not uncommon to find studies of gas phase polymerization that include only the principal components of a linear low-density polyethylene (LLDPE) experiment included in the experimental plan: ethylene, a comonomer, hydrogen and possibly nitrogen as process gases. It is often assumed that other components, such as alkanes used for heat transfer control are not important as they are chemically inert. However, in typical production processes the rate of heat generation during the polymerization is on the order of 1 MW per tonne of polymer in the reactor, meaning that the production rate will be limited by the amount of heat that can be removed from the reactor.<sup>[1]</sup> It is common industrial practice to add alkanes (often referred to as inert condensing agent – ICA – even if they are not condensed) such as propane, *iso*-butane, *iso*-pentane or *n*-hexane, either in vapour form (this is referred to as super dry operation), or (partially) liquefied in the case of condensed mode operation.

When compounds heavier than ethylene are present (either comonomer or ICA) they can have a certain number of different effects. Comonomers can obviously participate in the polymerization process and determine several final properties. However, these heavier compounds can also have a significant impact on the sorption and diffusion of ethylene and comonomers in the amorphous phase of the polymer.<sup>[2-4]</sup> The increased solubility leads to an enhancement of the rate of polymerization, and this is referred to as the cosolubility effect.<sup>[5-9]</sup> Not only does the cosolubility effect increase the rate of polymerization, it also influences the molecular weight distribution, particle morphology, crystallization rate and reactor behaviour.<sup>[10-14]</sup> Furthermore, it has been shown recently that ICA addition during copolymerization processes alters the polymer crystallinity with respect to similar copolymerizations performed without ICA due to competing cosolubility effects.<sup>[13]</sup>

While the isolated effect of each process variable is reasonably well understood, synergistic effects are not necessarily easily identified. For instance, it has been shown that, in certain cases, increasing the temperature of polymerization in the presence of an ICA can actually lead to a slight decrease in the rate of polymerization.<sup>[11]</sup> This observation was attributed to a competition between an increase in the rate of propagation with temperature (since the polymerization is an exothermic reaction) on the one hand, and a decrease in the impact of the cosolubility effect as temperature increases. As has been discussed elsewhere, there is a singular lack of data to fit semi-empirical equations of state to predict solubility,<sup>[15]</sup> and diffusivity,<sup>[16]</sup> in multicomponent system, and this makes it very difficult to predict

synergistic effects in olefin polymerizations. It is therefore useful to develop other methods of understanding these interactions in the absence of robust process models.

Clearly, understanding the synergetic effect of polymerization input variables such as temperature, monomer, comonomer and ICA pressure on polymerization kinetics, polymer yield and final polymer properties is important. The use of one-factor-at-a time (OFAT) experimental approach is not sufficient when considering several factors because the interactions between the input variables on the output variables are not clearly identifiable. The use of good design of experiment (DoE) tool can help to adequately capture and explain the impact of interactions between the various input variables on the output variables. One way of describing the polymerization process in the absence of fully defined mechanistic models is by using statistical modeling tools such as response surface methodology (RSM) and artificial neural network (ANN).

RSM is a collection of mathematical and statistical approaches for empirical model building. The response of interest depends on several significant variables, and the objective of the method is to model and optimize this response.<sup>[17]</sup> Its major benefit is its capacity to reduce the number of experiments needed to assess the effects of the input variables involve and their interaction on the output variables. Hence, mathematical models developed for a particular system based on RSM data have been found to be suitable with knowledge of the process, thus minimize the experimental cost as well as saves time,<sup>[18]</sup> and has been successfully applied in some polymerization processes.<sup>[19-24]</sup>

ANN is a data driven machine learning tool described as ‘black-box’ because information about the functional relationship between the input and the output variables is not necessarily needed.<sup>[25]</sup> It can adequately solve complex non-linear problems without previous knowledge of the system by capturing the relationship between input and output variables from a given process.<sup>[26]</sup> The framework of the ANN is the multi-layered perceptron (MLP) which comprised of input, hidden and output layers accompanied by “neurons” which may vary in number depending on the complexity of the process system to be used. ANN has also been used to study olefin polymerization processes.<sup>[26-31]</sup> In comparison to RSM, which is useful only for quadratic approximations, ANN can be used to approximate numerous kinds of non-linear functions plus quadratic functions.<sup>[32]</sup> In general, both RSM and ANN belong to modeling approaches that deals with developing non-parametric simulative models.<sup>[33]</sup> Some previous studies concluded that ANN gave better results than RSM<sup>[33-35]</sup> for certain non-polymerization processes, while other reports concluded the opposite.<sup>[36, 37]</sup> There did not appear to be any clear, general conclusion concerning which approach to use for the case of

interest here. And while RSM and ANN has separately been employed to model some polymerization processes, to the best of our knowledge, no study has compared the ability of both tools to provide insight into the impact of several process variables, and in particular ICAs, on polymerization kinetics, polymer yield and final polymer properties in gas phase ethylene polymerization.

We therefore used both ANN and RSM methods to analyse an experimental study of the impact of interactions between the main process variables in a gas phase polymerization process (ethylene, 1-butene and iso-pentane pressures, reactor temperature) on the rate of polymerization, catalyst deactivation, yield, the melt flow index (MFI) and polymer crystallinity. The 3D response surface plot of RSM was employed to study the synergetic effect of the studied input variables (reaction temperature, monomer and comonomer pressure) on polymerization maximum activity, ratio of maximum to minimum activity ( $A_{\max}/A_{60}$  – where  $A_{\max}$  and  $A_{60}$  refer to the maximum activity and the activity observed after the end of the 60 minute experiments) or deactivation, polymer yield and final polymer properties (crystallinity and melt flow index) while keeping the hydrogen pressure and reaction time constant at 1 bar and 60 min, respectively. The performance of these models is compared by employing statistical criteria such as determination coefficient ( $R^2$ ), adjusted  $R^2$ , root mean squares error (RMSE), and average absolute deviation (AAD).

## 2.0 Experimental section

### 2.1. Chemicals

Argon, hydrogen, and ethylene all with a minimum purity of 99.5%, were procured from Air Liquide (Paris, France). Ethylene was passed through three different purification columns before use: a first one packed with reduced BASF R3-16 catalyst (CuO on alumina), a second one filled with molecular sieves (13X, 3A, Sigma-Aldrich), and the last one loaded with Selexsorb COS (Alcoa). 1-butene having a minimum purity of 99% was obtained from Air Liquide. *Iso*-pentane with a minimum purity of 99% was obtained from Sigma-Aldrich ICN (Germany) and was further purified through distillation over  $\text{CaH}_2$ . The co-catalyst (Triethylaluminium) was obtained from Witco (Germany). All the polymerization reactions were performed using a commercial  $\text{TiCl}_4$  supported on  $\text{MgCl}_2$  Zeigler-Natta catalyst. NaCl with 99% minimum purity was obtained from Carl Roth (Germany) and used as seedbed to disperse the catalyst particles. The salt was dried under vacuum for 5 h at 400 °C before use to eliminate all the traces of water.

## 2.2. Polymerization procedure

Gas phase polymerization was performed in a 2.5 L spherical stirred-bed gas phase reactor at constant temperature following a procedure described elsewhere, using a seed bed of 40 grams of dried NaCl [12]. As the catalyst formulation was not included in the statistical analysis, all runs were run with 7 mg of Ziegler-Natta catalyst (mixed with 10 g NaCl in glovebox and transferred into cartridge) and 0.6 ml of a 1 M TEA solution in heptane. All polymerizations lasted for 60 minutes for a particular set of conditions. At the completion of the reaction, the reactor was depressurized and cooled. Product was retrieved and washed by water and then dried under vacuum at 70 °C. All the polymerization runs considered here, as well as the experimental measurements are summarized in Table 1 (N.B. the responses are in anticipation of the ANN results). Polymerization temperatures considered include 70, 80 and 90°C. The range of pressures considered are 7, 8 and 9 bars for ethylene (C2), and 0, 1, and 2 bars for both of 1-butene (1-C4) and *iso*-pentane (iC5). Hydrogen pressure was kept constant at 1 bar. The rates of polymerization are measured with the pressure drop in the feed ballast, and the value of the maximum activity ( $A_{\max}$ ) divided by the activity at 60 minutes ( $A_{60}$ ) is taken as an indicator of catalyst deactivation during the experiments. Yield was measured gravimetrically.

## 2.3. Polymer Characterization

DSC analysis was performed with a Mettler Toledo DSC 1 system equipped with an autosampler and a 120-thermocouple sensor. Indium standard was used to calibrate the temperature and the heat flow of the equipment. All polymer powders were accurately weighed ( $6 \pm 0.2$  mg) and sealed in aluminum pans of volume 40  $\mu$ L. The reference was an empty aluminum pan. The purging gas was dry nitrogen with a flow rate set at 50 mL/min. The data obtained were processed with STARE thermal analysis software. The temperature corresponding to the melting peak point is defined as melting peak temperature ( $T_m$ ). The crystallinity (by weight,  $w_c$ ) of the samples was estimated through  $w_c = \Delta H_f / \Delta H_{f0}$ , where  $\Delta H_f$  (J/g) is the melting enthalpy of the sample and  $\Delta H_{f0}$  (293 J/g) is the melting enthalpy of a 100% crystalline polyethylene. In the conventional DSC protocol, samples were heated to 180 °C to erase thermal history and then cooled to -20 °C before being heated to 180 °C (heating rate, 10 °C/min; cooling rate, -10 °C /min).

The ASTM D1238 test was utilized to determine the melt flow index (MFI) of the polymer powders using an extrusion MFI tester (Zwick Roell, Ulm, Germany). The polymer sample weighing approximately 5 g is melted at 190 °C with a mass of 21.6kg followed by extrusion. The extrudate is further weighed (precision scale of 0.001 g) and then normalized by melt flow time in this case 10 min to give the MFI value.

Table 1: BBD matrix of independent variables and experimental values for the polymerization process.

Run	Factor				Response				
	C2 (bar)	1-C4 (bar)	iC5 (bar)	Temp (°C)	MFI (g/10 min)	$\chi$ (%)	Yield (kg PE/g cat)	A <sub>max</sub> (kg PE/g cat.h)	A <sub>60</sub> (kg PE/g cat.h)
1	8	0	1	70	1.2	67	1.6	6.8	0.8
2	8	0	1	90	2.5	70	1.2	4.4	0.6
3	8	1	1	80	3.6	49	4.1	14.7	1.7
4	7	1	1	90	15.6	48	1.1	3.7	0.5
5	8	1	1	80	3.9	50	4.2	14.4	1.7
6	7	1	1	70	3.4	48	2.5	15.2	1.2
7	9	1	1	90	11.2	47	2.9	8.4	1.3
8	8	1	1	80	3.8	50	4.3	14.2	1.7
9	8	1	0	90	8.5	50	2.4	4.4	0.5
10	8	1	2	70	2.4	50	4.1	17.1	1.7
11	8	1	0	70	3.9	50	3.3	12.3	1.6
12	8	0	0	80	2.4	67	1.3	5.0	0.6
13	8	2	2	80	6.1	41	6.8	19.8	5.9
14	7	2	1	80	11.0	36	3.4	12.2	2.0
15	7	1	0	80	8.7	47	2.4	9.6	1.2
16	9	0	1	80	1.3	67	1.5	9.9	1.2
17	7	0	1	80	1.4	64	2.5	8.4	0.9
18	7	1	2	80	3.4	49	3.6	9.9	1.3
19	8	0	2	80	1.1	69	2.2	9.6	1.5
20	8	1	1	80	3.7	50	4.0	14.2	1.7
21	8	2	1	90	11.2	44	4.7	16.8	2.0
22	9	1	0	80	2.2	46	4.0	14.9	1.3
23	9	1	2	80	1.9	48	2.4	17.1	3.8
24	8	1	2	90	3.2	52	3.4	11.0	2.1
25	8	2	0	80	11.0	36	4.8	18.6	2.4
26	9	2	1	80	2.9	32	6.3	22.8	3.6
27	8	2	1	70	7.9	36	5.4	18.4	2.9
28	9	1	1	70	3.1	48	3.4	16.2	1.9

C2 – ethylene, 1-C4 – 1-butene, iC5 – *iso*-pentane, Temp – temperature,  $\chi$  – crystallinity

### 3.0 Model development

#### 3.1 Development of RSM model

A three-level-four factor Box Behnken design (BBD) of RSM was employed in the modeling of the gas phase polymerization of ethylene and 28 experimental conditions were generated (c.f. Table 1). The center point was repeated four times to determine the repeatability of the method. To relate the response variable to the four independent variables, multiple regressions were used to fit the coefficient of the quadratic polynomial model of the response. The quality of the fitted model was evaluated using a test of significance and analysis of variance (ANOVA). Equation (1) describes the fitted quadratic response model:

$$Y = \Omega_0 + \sum_{i=1}^n \tau_i \Omega_i + \sum_{i=1}^n \tau_{ii} \Omega_i^2 + \sum_{i=1}^n \sum_{j=1}^n \tau_{ij} \Omega_i \Omega_j + \epsilon \quad (1)$$

where  $Y$  is response variable,  $\Omega_0$  is the intercept value,  $\tau_i$  ( $i = 1, 2, \dots, n$ ) is the first order model coefficients for  $\Omega_i$ ,  $\tau_{ij}$  is the interaction coefficients for  $\Omega_i \Omega_j$ , and  $\tau_{ii}$  represents the quadratic coefficients of  $\Omega_i$ , and  $\epsilon$  is the random error.

#### 3.2 Development of ANN model

A Levenberg–Marquardt (LM) algorithm with feedforward backpropagation having two layers, also known as multilayered perceptron (MLP), was selected for this present study. The weighted inputs and the corresponding bias are summed up by setting the neurons in the hidden layer as shown in equation (2). This consequently directs the input data across a more nonlinear system. The hyperbolic tangent sigmoid transfer function (*tansig*) and purelin transfer functions were employed for the input and output layers, respectively. These transfer functions were used to formulate the activation function as illustrated in equation (3). Also, equation (4) shows the net input to the output layer node.

$$\theta_j = \sum_{k=1}^r I_k \omega_{jk}^{in} + \beta_j^{in} \quad (2)$$

$$f(x) = \text{tansig}(x) = \frac{1 - e^{-x}}{1 + e^{-x}} \quad (3)$$

$$I_u = \sum_{j=1}^s f(\theta_k) W_{uj}^{out} + \beta_u^{out} \quad (4)$$

where  $\theta_j$  is the node  $j$  net input in the hidden layer,  $I_k$  is the input to a node  $k$ ,  $\omega_{jk}^{in}$  denotes the weight linked with every single input connection from  $k$ th to  $j$ th neuron in the hidden layer. The bias of the  $j$ th neuron in the hidden layer is denoted by  $\beta_j^{in}$  while the net input to the node  $u$  in the output layer is denoted by  $I_u$ . The weight connecting neuron in the hidden layer from  $j$ th to  $u$ th neuron in the output layer is represented by  $W_{uj}^{out}$  while the bias of the  $u$ th neuron in the output layer is denoted by  $\beta_u^{out}$ . Neuron numbers in the input, hidden and output layers are represented by  $r$ ,  $s$ ,  $u$ .

In the present study, despite the fact that the input-output variables follow the *multiple in multiple output* (MIMO) type, a *multiple input single output* (MISO) approach was used to setup the ANN architecture. The MIMO architecture consists of a single neural network where all the responses are simulated simultaneously with multiple inputs.<sup>[38]</sup> Obviously, MIMO architecture unarguably simplifies the ANN model development. However, in some cases the output variables can depend on the multiple input variables, or they can possibly depend on the same inputs, the convergence criteria to compute the weights and biases in the training phase and the output adjustment can be randomly favoured.<sup>[39]</sup> Hence, these problems can be overcome by employing MISO architecture, but the same neural network as the outputs must be developed.

The proposed model has four networks, and each has an input layer with four neurons (reaction temperature, ethylene, 1-butene and *iso*-pentane pressure), a hidden layer and an output layer with one neuron for a particular response (MFI, yield, maximum activity, deactivation or crystallinity). The network topology was based on the number of hidden neurons selected. The optimum number of hidden neurons was chosen by trial-and-error or heuristic procedure. Hidden neurons which ranged from 2 - 20 were tested iteratively until mean square error (MSE) attained a minimum value for each network. Overfitting of the model for each network was checked for the dataset containing the responses and the process input variables by dividing the dataset into three subsets: training (~70%), validating (~15%) and testing (~15%). Table 2 illustrates the parameters employed for developing ANN for each network. MATLAB's Neural Network in MATLAB R2018a (MathWorks Inc., Natick, MA, USA) was employed for the modeling exercise.

Table 2: Features of ANN model

Model	Property	Value/Comment
ANN	Algorithm	Levenberg-Marquardt back-propagation
	Minimised error function	MSE
	Learning	Supervised
	Input layer	No transfer function is used
	Output layer	Purelin
	Hidden layer	Hyperbolic tangent sigmoid (tansig)
	Number of training iterations	100
	Number of best iterations	70
	Number of input neurons	4 <sup>a</sup>
	Number of hidden neurons	2-20
Number of output neurons	5 <sup>b</sup> (1 neuron for each network)	

<sup>a</sup>Independent variables

<sup>b</sup>Dependent variables

The ANN model does not directly give insight into the system because it uses a ‘black-box’ approach. Hence, a sensitivity analysis of the system is needed to determine the relative importance of each input variable on a particular output variable. An equation depicting how to compute the relative importance of each input variable on the output variable based on the weight partitioning was developed by Garson.<sup>[40]</sup> This equation is given as:

$$\lambda_j = \frac{\sum_{m=1}^{m=n_h} \left( \left( \frac{|W_{jm}^{ih}|}{\sum_{k=1}^{n_i} |W_{km}^{ih}|} \right) \times |W_{mn}^{ho}| \right)}{\sum_{k=1}^{k=n_i} \left\{ \sum_{m=1}^{m=n_h} \left( \frac{|W_{km}^{ih}|}{\sum_{k=1}^{n_i} |W_{km}^{ih}|} \right) \times |W_{mn}^{ho}| \right\}} \quad (5)$$

where,  $n_i$  and  $n_h$  denote the number of input and hidden neurons, respectively. The connection weight is denoted by  $W$  and the superscripts  $i$ ,  $h$  and  $o$  denote the input, hidden, and output

layers, respectively; subscripts  $k$ ,  $m$  and  $h$  denote input, hidden and output neurons, respectively.  $\lambda_j$  is the relative importance of the  $j$ th input variable on the output variable.

### 3.3 Statistical evaluation of the developed RSM and ANN models

The predictive capability of the two developed models were assessed statistically. This was done by using various statistical indicators such as coefficient of determination ( $R^2$ ), adjusted  $R^2$ , average absolute deviation (AAD), and standard error of prediction (SEP). The obtained results were compared to establish which of the models is superior to the other. Equations (6)-(9) were used to compute these indicators.

$$R^2 = \frac{\sum_{i=1}^n (x_{i,ob} - x_{i,pr})^2}{\sum_{i=1}^n (x_{i,pr} - x_{ob,m})^2} \quad (6)$$

$$Adjusted\_R^2 = 1 - \left[ (1 - R^2) \times \frac{n - 1}{n - v - 1} \right] \quad (7)$$

$$RMSE = \sqrt{\frac{1}{n} \sum_{i=1}^n (x_{i,pr} - x_{i,ob})^2} \quad (8)$$

$$AAD = \frac{100}{n} \sum_{i=1}^n \frac{|(x_{i,ob} - x_{i,pr})|}{x_{i,ob}} \quad (9)$$

where  $n$  is the number of experimental data,  $x_{i,pr}$  is the predicted values,  $x_{i,ob}$  is the experimental values,  $x_{ob,m}$  is the average experimental values and  $v$  is the number of input variables.

## 4.0 Results and Discussion

### 4.1 RSM based Predictive Model.

The predicted results of the various independent variables studied of the developed response surface quadratic models are shown in Table S1 in the supporting information. While it is possible to use linear, quadratic and cubic models in the RSM approach, the quadratic model was selected due to its capability to adequately represent the gas phase polymerization process (higher order models were tested but did not bring any improvement in terms of process understanding). In fact, the criterion for the model selection was based on choosing the highest polynomial model, that has additional significant term in which the model is not

aliased. The ANOVA results which show the linear, interactive, and quadratic relationship between the effects of independent variables on dependent variables is described in Figures 1a-e (Pareto chart) for all the five independent variables considered. The Pareto chart were developed using Statistica 13 software (StatSoft Inc., Tulsa, OK, USA) to ascertain the level of the significance of each term and their respective interactions. From the chart, any bar that finishes to the left of the reference line ( $p < 0.05$ ) is considered statistically insignificant and included in the empirical model. The quadratic regression models obtained for the process for all 5 responses are shown by equations S1 (see supporting information) in the supplementary material. The coefficients for each term are indicated at the end of each bar. Obviously, the higher the coefficient, the more significant the impact of the independent variable is on the output considered. Similarly curved surfaces reflect a non-linear relationship between input and output variables.

If one considers the response surface plots of the MFI seen in Figure 2 as an example, it can be seen (as one would expect) that each of the linear terms seem to be quite important in determining the value of the MFI, with the 1-C4 pressure apparently having the greatest impact over the range studied, and the iC5 pressure having the smallest. This can be seen from the shapes of the surfaces in said Figure. The explanations for these observations are straightforward. Increasing the 1-C4 pressure and the temperature both lead to an increase in the MFI (i.e. a decrease in the viscosity average molecular weight) as one would expect with a Ziegler-Natta catalyst. Increasing the C2 pressure causes a decrease in the MFI as higher ethylene concentrations generally lead to higher molecular weights with Ziegler-Natta catalysts. Increasing iC5 decreases the MFI since higher ICA pressures provoke a greater solubility (and diffusivity) of C2 in the amorphous phase of the polymer covering the active sites, and thus also contributes to a higher molecular weight. Except for the impact of the terms on catalyst deactivation, the explanations of the impact of the first order terms of the independent variables on the other output variables are also straightforward so we will not discuss them further in this paper. It is not immediately clear why each of the independent variables studied have a negative correlation with the deactivation, however it is very interesting to note that while all of these variables positively impact the maximum activity, they have a negative impact on the deactivation. Clearly, this subject merits more extensive investigation.

The degree and nature of the impact of independent variables can also be seen from the response surfaces for the crystallinity, the one-hour yield, the maximum activity, and the deactivation ( $A_{\max}/A_{60}$ ) can be seen in Figures S1-S4 in the supporting information.

On the other hand, the interactions between variables (i.e. the cross terms in the quadratic model) are not so evident without looking more closely at this statistical analysis. The statistically significant interactions between independent variables are shown in Table 3.

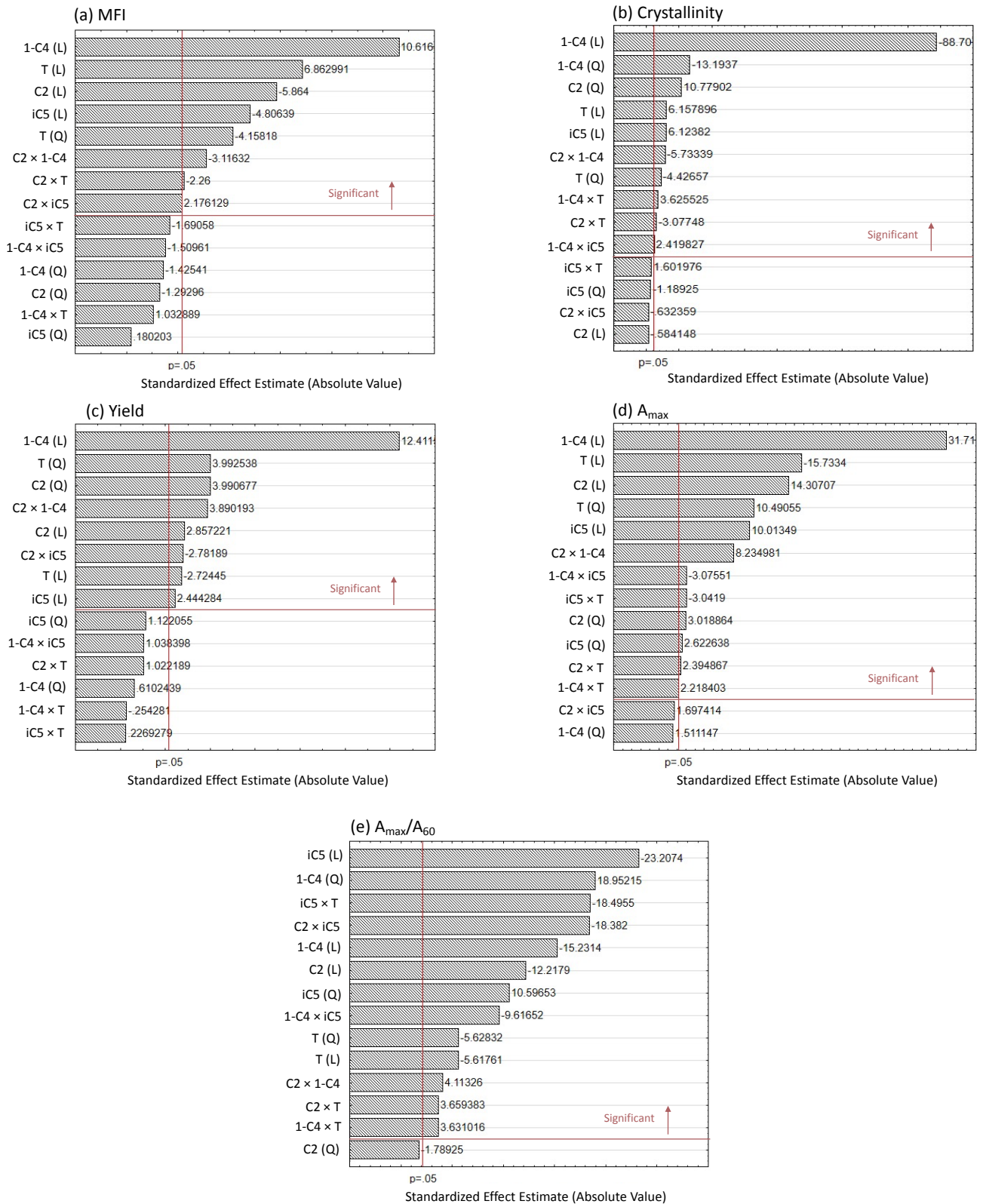
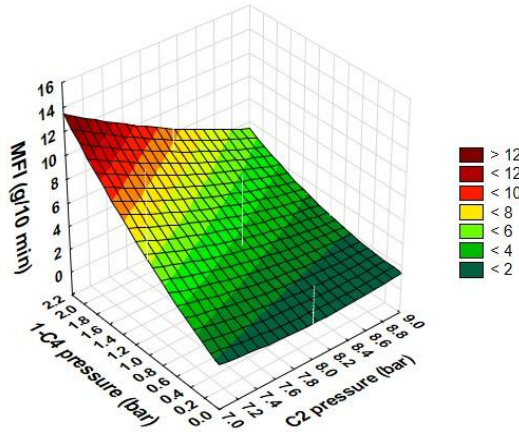
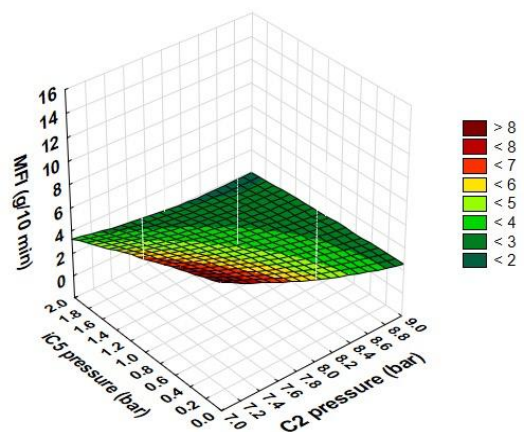


Figure 1: Pareto diagram of standard effect for the RSM model: (a) MFI; (b) crystallinity; (c) yield; (d) maximum activity; (e) Deactivation (maximum activity divided by activity at 60 min. L represents 1<sup>st</sup> order (linear) terms, Q represents 2<sup>nd</sup> order (quadratic) terms.

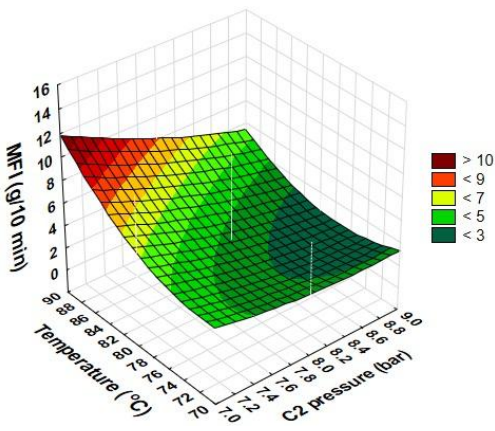
(a) C2 × 1-C4



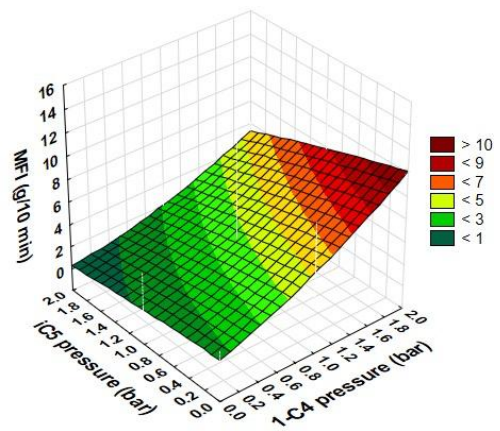
(b) C2 × iC5



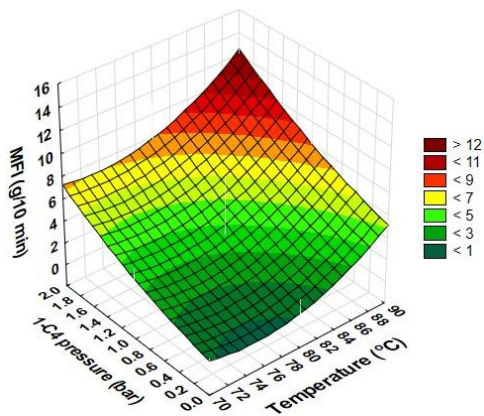
(c) C2 × T



(d) 1-C4 × iC5



(e) 1-C4 × T



(f) iC5 × T

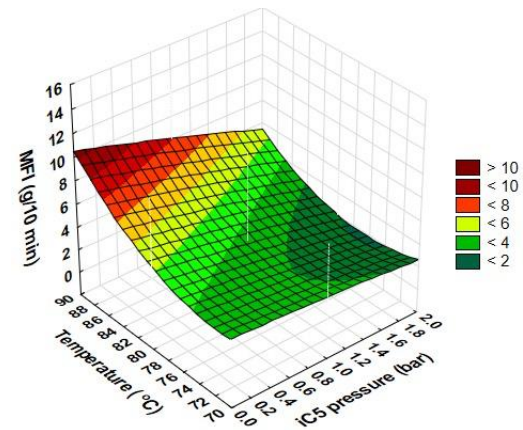


Figure 2. Response surfaces for the MFI as a function of the indicated process variables.

Table 3. Statistically significant interactions between independent variables on the studies properties.

Interaction	MFI	Crystallinity	Yield	$A_{\max}$	$A_{\max}/A_{60}$
C2 × 1-C4	X	X	X	X	X
C2 × iC5	X		X		X
C2 × T	X	X		X	X
1-C4 × iC5		X		X	X
1-C4 × T		X		X	X
iC5 × T					X

The set of results seen in Table 3 are difficult to interpret fully without significantly more experiments – on the other hand identifying this type of hidden interaction worthy of more detailed study is really the point of the statistical analysis in this case. However, one point is abundantly clear: catalyst deactivation is a very complex issue, and appears to be impacted by the entire set of independent variables chosen here, both linearly, and via different interactions (the only statistically insignificant term in the process model would be the quadratic term of ethylene pressure). It is unlikely that one can attribute enhanced deactivation to particle heating, as increasing the temperature also increases the yield (and thus average polymerization rate.) It could be proposed that perhaps trace amounts of inhibitor not removed in the purification columns could be the culprit for the higher deactivation being correlated with higher maximum activity. Given that the lab reactor is in semi-batch mode, increasing the rate of polymerization increases the rate of ethylene feed to keep the pressure constant. In this case, if the feed is not perfectly pure, then increasing the ethylene feed rate might lead to an accumulation of trace amounts of poisons in the gas phase that could, in turn, lead to faster deactivation. As we mentioned above, this analysis shows that it is important to study the factors contributing to deactivation in much greater detail.

The results in Table 3 also reveal that the presence of at least one alkane is far from anodyne. Previous results from our group have shown that this is the case, but it can also be seen that iso-pentane has significant interactions with the other process parameters on both the polymerization kinetics, and the polymer properties. The implications of this are that the study of the impact of the choice of induced condensing agents in gas phase polymerization is not straightforward, nor can we ignore these chemically inert materials in developing process models.

Once again, the purpose of the current paper is not to explain these complex interactions, but rather to attempt to show that a RSM is a useful technique for eventually

building an empirical process model (e.g. for process control purposes), but also for identifying potentially important directions for future experimental research. It remains to be seen if the same type of information can be obtained from ANN methods.

#### **4. ANN based predictive model.**

The ANN optimum topology in this study was based on two steps which include optimal number of neuron selection and testing/validation/training of the model. Neurons in the range of 2-20 were selected for the estimation and prediction of polymer yield, maximum activity, deactivation, and final polymer properties. This is because the selection of an optimal neural network topology is important to successfully employ ANN.<sup>[41]</sup> The determination of the optimum number of neurons was based on the heuristic procedure in which the MSE for training, validation and testing had the lowest values and the *R* showed the highest value as illustrated in Figures 3a-e. From the plots, it appears that 10 neurons had the lowest MSE and highest *R* values. Hence, the topology of the developed ANN for each response is 4-10-1. This topology translates to three layers as input layer with four input variables (temperature, ethylene, 1-butene and iso-pentane pressure), a hidden layer with ten hidden neurons (as determined heuristically), and an output layer with single output variable (either MFI, or crystallinity, or yield, or maximum activity, or Amax/A60). The prediction for each of the responses is shown in Table S1. The plots of the predicted values versus the target values for the training, validation, testing, and entire datasets is shown in Figure S5 of the supporting information.

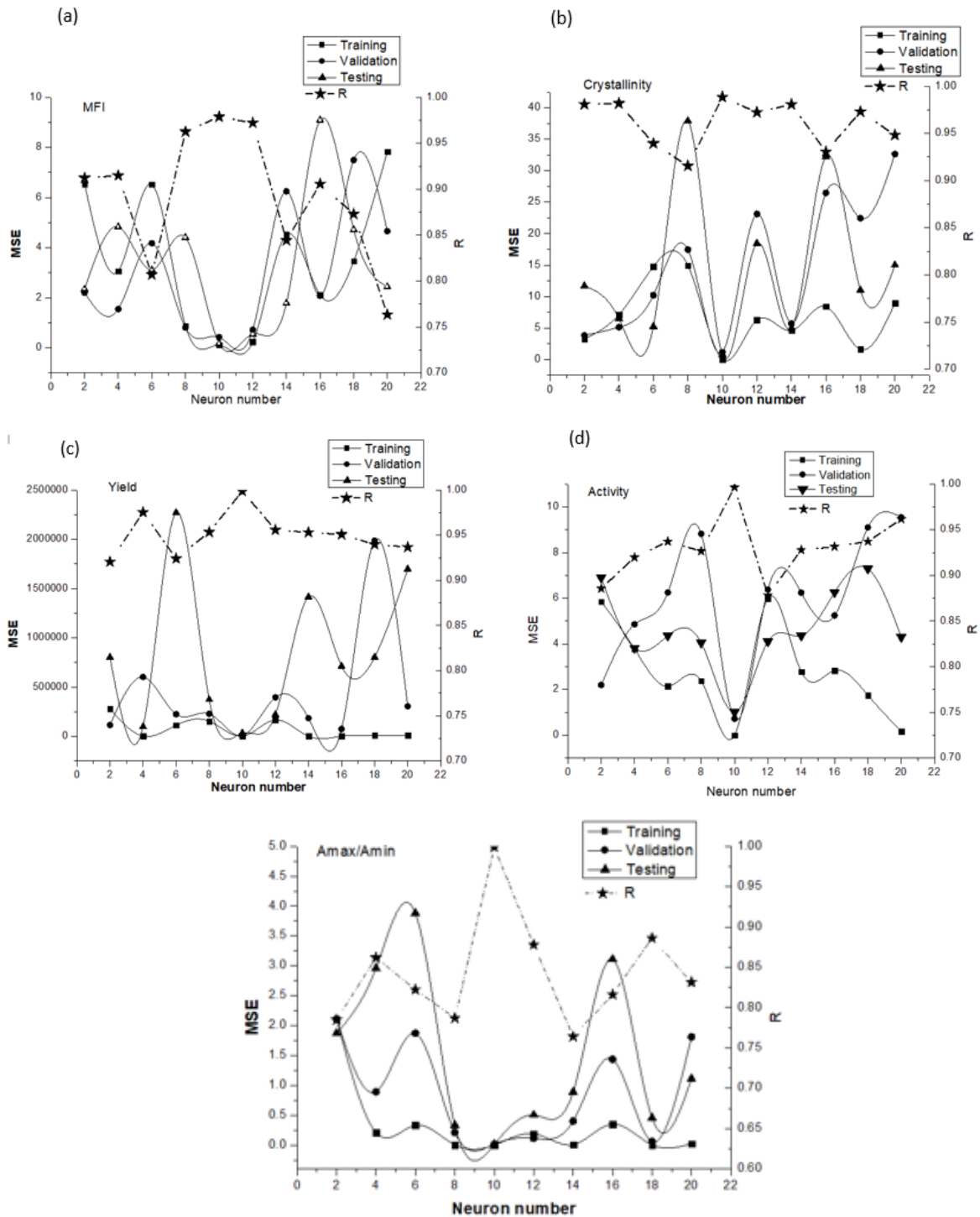


Figure 3: Optimal number of hidden neurons for all the responses studied.

The weights computed for both the inputs and output variables from the developed ANN model are listed in Table S2 (supporting information). The relative importance of the studied four input variables calculated by employing Equation 5, Garson,<sup>[40]</sup> on each of the responses is shown in Figures 4a-e. If one compares this Figure to the linear values of the input variables in Figure 1, the ANN predicts a very similar hierarchy of importance of the inputs

on each output variable, with the exception of the crystallinity, where the order of importance is somewhat different. Note that as the histograms in Figure 1 include the values of the quadratic and interactive terms, one cannot directly compare the relative importance generated with the ANN in Figure 4 and the relative size of the histograms in Figure 1. The 3D surface plot was also plotted for the developed ANN model. This is done by extracting the predicted values from the MATLAB and generating the 3D surface plot for a particular response. The 3D surface plots by ANN are shown in Figure S11 of the supporting information.

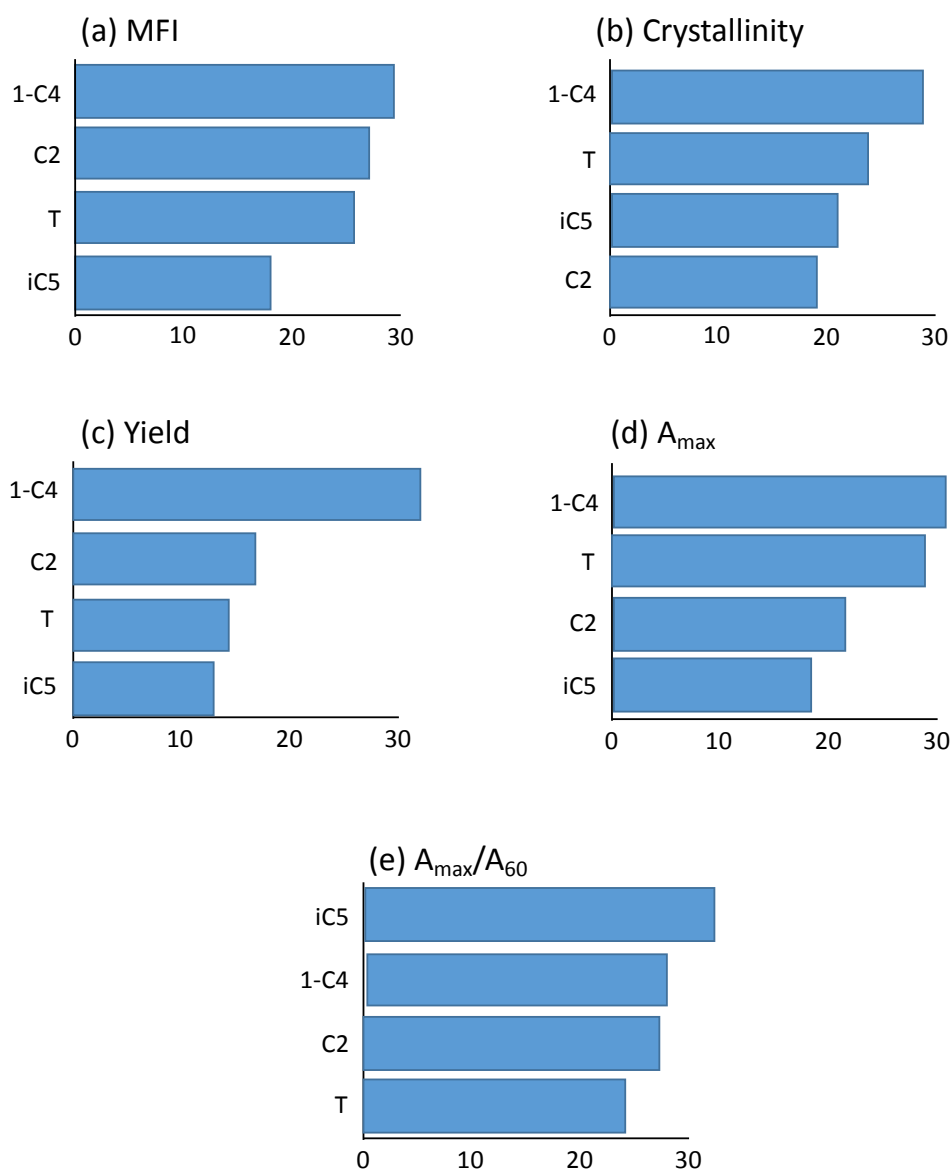


Figure 4: Level of importance of process input variables on the different output variables.

The developed RSM and ANN models were compared to ascertain their general performance. The comparison was based on various statistical parameters ( $R^2$ , adjusted  $R^2$ , RMSE and AAD). Table 4 shows the comparative values of these statistical parameters while Figures 5a-e shows the comparison plots for the actual and predicted values of all the responses for the developed models. Table 4 shows that both models performed effectively, but the developed ANN model was slightly better than the developed RSM model. Furthermore, a comparison of Figures 2 and S1-S4 to Figures S7-S11 show that the surface responses of the two approaches are also very similar. The table shows that the computed  $R^2$  and adjusted  $R^2$  values for ANN model are slightly higher than that of RSM model while the computed error analysis values (RMSE and AAD) for ANN are slightly lower than that of RSM model. The differences between the two methods are very slight. This in turn suggests that the extra effort required to develop and tune the ANN models is not worth the investment.

Table 4: Performance evaluation of RSM and ANN models

	<b>MFI</b>		<b>Crystallinity</b>		<b>Yield</b>		<b>Activity</b>		<b><math>A_{max}/A_{60}</math></b>	
	<b>RSM</b>	<b>ANN</b>	<b>RSM</b>	<b>ANN</b>	<b>RSM</b>	<b>ANN</b>	<b>RSM</b>	<b>ANN</b>	<b>RSM</b>	<b>ANN</b>
$R^2$	0.953	0.977	0.998	0.991	0.946	0.978	0.993	0.993	0.994	0.998
Adj $R^2$	0.945	0.974	0.998	0.980	0.937	0.975	0.992	0.992	0.994	0.997
RMSE	0.772	0.547	0.441	1.481	336.3	213.53	0.405	0.416	0.120	0.084
AAD	14.44	8.494	0.652	1.596	11.03	5.53	3.40	2.72	1.35	0.397

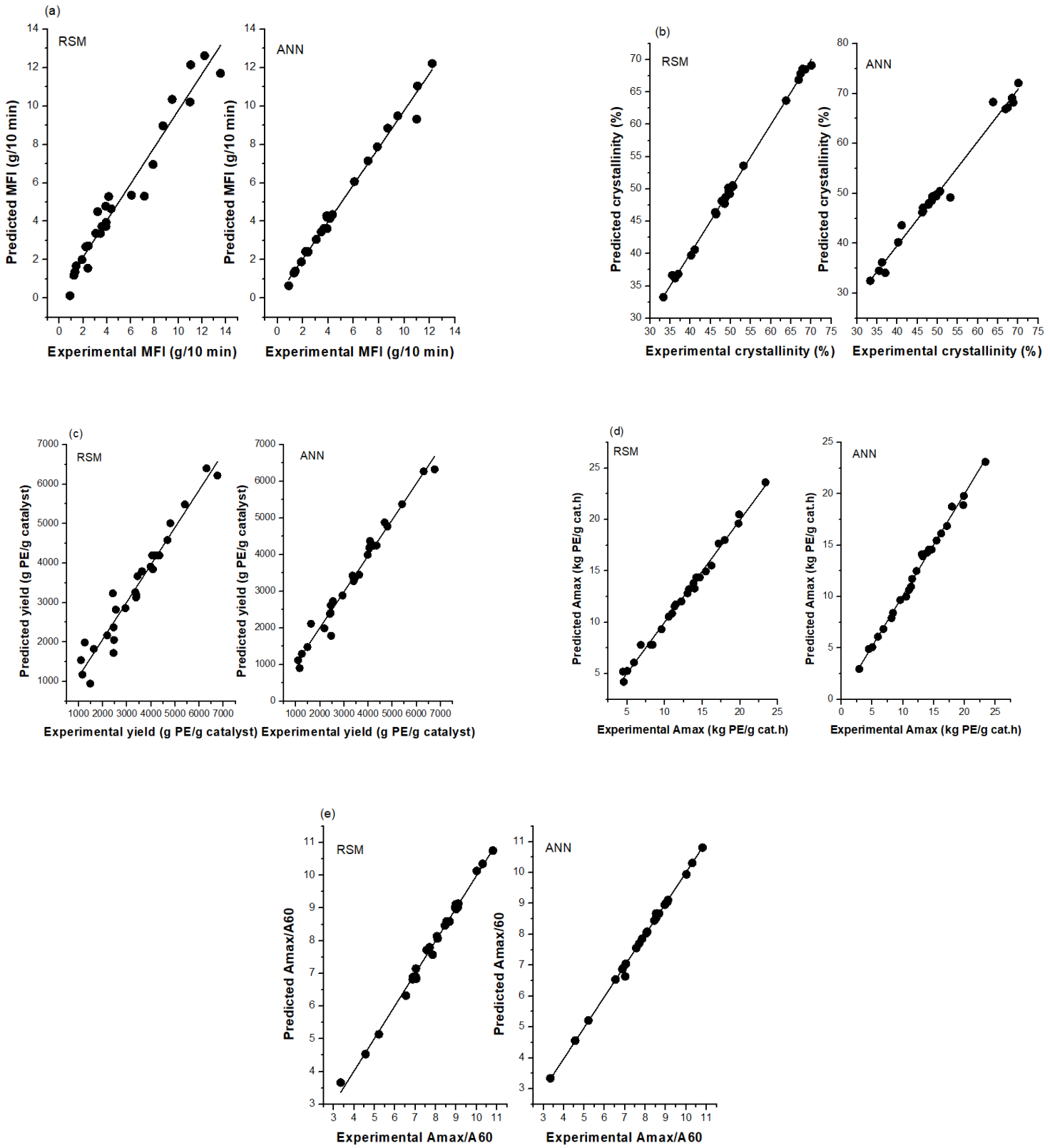


Figure 5: Experimental versus predicted values parity plots for (a) MFI (b) Crystallinity (c) yield (d) maximum activity

## Conclusion

Gas phase ethylene/1-butene copolymerization with a commercial ZN catalyst in the presence of *iso*-pentane as ICA has been investigated in this study. Experimental results showed that the presence of ICA has impact on the polymerization kinetics and final polymer properties (MFI and crystallinity). In this study, RSM and ANN were employed for modeling the gas phase ethylene/1-butene copolymerization. The BBD of RSM was used to design the experiment and the dataset generated were used to develop the RSM and ANN models. The regression equations in actual terms were calculated by RSM to illustrate the functional empirical relationship between the independent variables (ethylene, 1-butene, *iso*-pentane pressure and reaction temperature) and the dependent variables. Both developed models were statistically analysed in order determine their performance ability. The developed ANN model was slightly better than the developed RSM model based on these statistical parameters ( $R^2$ , adjusted- $R^2$ , RMSE and AAD) due to its ability to capture the nonlinear behaviour of the system. The sensitivity analysis of the developed ANN model showed that all the studied input variables have significant impact on the studied responses. In contrast to the opinion that for effective ANN model, a much greater number of experimental runs is required than RSM, the results obtained in this present study show that an effective ANN model can be built from a method of an RSM screening approach such as BBD.

## Acknowledgement

NBI acknowledges funding support from Petroleum Technology Development Fund (PTDF), Nigeria for the doctoral scholarship (Grant Number: 18GFC/PHD/064).

## References

- [1] J. A. Moebus, B. R. Greenhalgh, *Macromolecular Reaction Engineering* **2018**, *12*, 1700072.
- [2] A. Alizadeh, M. Namkajorn, E. Somsook, T. F. McKenna, *Macromolecular Chemistry and Physics* **2015**, *216*, 903.
- [3] A. Alizadeh, M. Namkajorn, E. Somsook, T. F. McKenna, *Macromolecular Chemistry and Physics* **2015**, *216*, 985.
- [4] M. Namkajorn, A. Alizadeh, E. Somsook, T. F. McKenna, *Macromolecular Chemistry and Physics* **2014**, *215*, 873.
- [5] B. J. Banaszak, D. Lo, T. Widya, W. H. Ray, J. J. de Pablo, A. Novak, J. Kosek, *Macromolecules* **2004**, *37*, 9139.
- [6] A. B. Mrad, N. Sheibat-Othman, J. Hill, M. Bartke, T. F. McKenna, *Chemical Engineering Journal* **2020**, 127778.
- [7] S. K. Nath, B. J. Banaszak, J. J. de Pablo, *Macromolecules* **2001**, *34*, 7841.
- [8] A. Novak, M. Bobak, J. Kosek, B. J. Banaszak, D. Lo, T. Widya, W. Harmon Ray, J. J. de Pablo, *Journal of applied polymer science* **2006**, *100*, 1124.
- [9] W. Yao, X. Hu, Y. Yang, *Journal of applied polymer science* **2007**, *104*, 3654.
- [10] R. Alves, M. A. Bashir, T. F. McKenna, *Industrial & Engineering Chemistry Research* **2017**, *56*, 13582.
- [11] F. N. Andrade, R. Fulchiron, F. Collas, T. F. McKenna, *Macromolecular Chemistry and Physics* **2019**, *220*, 1800563.
- [12] F. N. Andrade, T. F. McKenna, *Macromolecular Chemistry and Physics* **2017**, *218*, 1700248.
- [13] N. B. Ishola, F. N. Andrade, F. Machado, T. F. McKenna, *Macromolecular Reaction Engineering* **2020**, *14*, 2000021.
- [14] M. Namkajorn, A. Alizadeh, D. Romano, S. Rastogi, T. F. McKenna, *Macromolecular Chemistry and Physics* **2016**, *217*, 1521.
- [15] A. Ben Mrad, S. Norsic, N. Sheibat-Othman, T. F. McKenna, *Industrial & Engineering Chemistry Research* **2021**.
- [16] R. F. Alves, T. F. McKenna, *Chemical Engineering Journal* **2020**, *383*, 123114.
- [17] DC. Montgomery, *Design and Analysis of Experiment*. John Wiley & Sons, **2008**.
- [18] M. Shanmugaprakash, V. Sivakumar, *Bioresource technology* **2013**, *148*, 550.
- [19] M. Ahmadi, R. Jamjah, M. M. NEKOU, G. H. ZHOUREI, H. ARABI, **2007**.
- [20] P. J. DesLauriers, J. S. Fodor, S. Mehdiabadi, V. Hegde, J. B. Soares, *Macromolecular Reaction Engineering* **2020**, *14*, 2000023.
- [21] P. J. DesLauriers, J. S. Fodor, J. B. Soares, S. Mehdiabadi, *Macromolecular Reaction Engineering* **2018**, *12*, 1700066.
- [22] S. Mehdiabadi, J. B. Soares, J. Brinen, *Macromolecular Reaction Engineering* **2017**, *11*, 1600044.
- [23] H. Nassiri, H. Arabi, S. Hakim, S. Bolandi, *Polymer bulletin* **2011**, *67*, 1393.
- [24] K. V. Pontes, M. Wolf Maciel, R. Maciel, M. Embiruçu, *Brazilian Journal of Chemical Engineering* **2011**, *28*, 137.
- [25] S. Sivanandam, S. Deepa, "Introduction to neural networks using Matlab 6.0", Tata McGraw-Hill Education, 2006.
- [26] S. Anantawaraskul, N. Chokputtanawuttlerd, "Estimation of Average Comonomer Content of Ethylene/1-Olefin Copolymers Using Crystallization Analysis Fractionation (Crystaf) and Artificial Neural Network (ANN)", in *Macromolecular symposia*, Wiley Online Library, 2009, p. 282/150.
- [27] M. Ahmadi, M. Nekoomanesh, H. Arabi, *Macromolecular theory and simulations* **2009**, *18*, 195.
- [28] T. Charoenpanich, S. Anantawaraskul, J. B. Soares, *Macromolecular Reaction Engineering* **2016**, *10*, 215.
- [29] T. Charoenpanich, S. Anantawaraskul, J. B. Soares, *Macromolecular Theory and Simulations* **2017**, *26*, 1700042.

- [30] Y. Mohammadi, M. R. Saeb, A. Penlidis, E. Jabbari, P. Zinck, F. J. Stadler, K. Matyjaszewski, *Macromolecular Theory and Simulations* **2018**, 27, 1700106.
- [31] B. A. Rizkin, R. L. Hartman, *Chemical Engineering Science* **2019**, 210, 115224.
- [32] M. Mansour Ghaffari, K. Mostafa, *Food and Nutrition Sciences* **2011**, 2011.
- [33] A. N. Sarve, M. N. Varma, S. S. Sonawane, *RSC Advances* **2015**, 5, 69702.
- [34] K. A. Patel, P. K. Brahmhatt, *Procedia Technology* **2016**, 23, 391.
- [35] S. S. Selvan, P. S. Pandian, A. Subathira, S. Saravanan, *Arabian Journal for Science & Engineering (Springer Science & Business Media BV)* **2018**, 43.
- [36] T. F. Awolusi, O. L. Oke, O. O. Akinkurolere, O. D. Atoyebi, *Cogent engineering* **2019**, 6, 1649852.
- [37] S. Ray, M. Haque, T. Ahmed, T. T. Nahin, *Journal of King Saud University-Engineering Sciences* **2021**.
- [38] R. Gareta, L. M. Romeo, A. Gil, *Energy conversion and management* **2006**, 47, 1770.
- [39] G. Mihalakakou, M. Santamouris, A. Tsangrassoulis, *Energy and buildings* **2002**, 34, 727.
- [40] D. G. Garson, **1991**.
- [41] E. S. Elmolla, M. Chaudhuri, M. M. Eltoukhy, *Journal of hazardous materials* **2010**, 179, 127.